J. Fluid Mech. (1990), *vol.* 218, *pp.* 483–508
Printed in Great Britain

Collapse in conical viscous flows

By M. A. GOLDSHTIK AND V. N. SHTERN
Institute of Thermophysics, Novosibirsk 630090, USSR

(Received 12 October 1988 and in revised form 21 September 1989)

A class of steady conically similar axisymmetrical flows of viscous incompressible fluid is studied. The motion is driven by a vortex half-line or conical vortex in the presence of a rigid conical wall or in free space. The dependence of the solutions on parameters (say, the vortex circulation) is analysed. At some finite parameter values the solutions lose existence, i.e. a flow collapse takes place. This is correlated with the appearance of a sink singularity at the symmetry axis. Analytical estimates of the critical parameter values are performed, together with numerical calculations of bounds on the solution existence region in parameter space.

Asymptotic analysis of the near-critical regimes shows that a strong axial jet develops. The jet momentum becomes infinite at the critical parameter value and a singularity occurs. These paradoxical features seem to be typical of conically similar viscous flows. Reasons for the paradox and ways of overcoming it are discussed. Solution non-uniqueness and a hysteresis phenomenon are found in the Serrin problem. Possible applications of the results to model some geophysical and astrophysical phenomena are outlined.

1. Introduction

Here we shall deal with a class of conically similar solutions of the Navier–Stokes equations. In this class, the velocity field is inversely proportional to the distance from the origin. Investigation of the class has a rather long and interesting history. The two-dimensional case was first studied by Jeffery (1915) and Hamel (1916). A variety of non-trivial features, such as non-uniqueness of steady solutions and the impossibility of divergent flow everywhere, was found when the Reynolds number was sufficiently large.

Generalization of the class to the three-dimensional case was done by Slezkin (1934). Then Landau (1944), Yatseev (1950) and Squire (1952) found exact solutions for the class. With the exception of the Landau jet, there were some difficulties in the interpretation of the other solutions. Because of the unusual properties of the solutions, the discussion has been continued up to the present (Schneider 1981, 1985; Goldshtik & Shtern 1987, 1988, 1989). The most intriguing property seems to be a loss of solution existence at some parameter value, due to the appearance of a singularity.

This effect was first found, and mathematically proved, in a problem on the interaction between a line vortex and a plane wall (Goldshtik 1960). When a circulation value increases, the axial and angular momenta are concentrated near the symmetry axis and at a finite circulation value a regular solution of the initial problem loses its existence.

Serrin (1972) has generalized the problem, allowing a logarithmic singularity of the longitudinal velocity at the symmetry axis. If a parameter P characterizing the

logarithmic singularity is chosen in a special way, then the solution may be continued up to an arbitrarily large value of circulation Γ_1. Serrin has calculated the solution existence boundary in the plane (P, Γ_1). Here it is found that the Serrin problem has more than one solution in some parameter subregion. Further, it is shown that a part of the Serrin boundary (for $P > 1$) correlates with the loss of existence due to the appearance of the sink singularity, but the other part (for $P < 1$) corresponds to merging and annihilation of two regular solutions of the initial-boundary problem. The second solution, having a two-cell flow structure, also loses its existence at lower P values due to singularity appearance. The problem is generalized to the case of a conical wall with arbitrary angle.

The collapse phenomenon is inherent in the Squire solution and its generalization for swirling flows (Goldshtik 1979; Yih *et al.* 1982). Squire interpreted his solution as a jet emerging from a hole in a plane wall. But some theoretical (Schneider 1981, 1985) and experimental (Zauner 1985) results testify that this interpretation is wrong. Here, the Squire solution is considered as a jet produced by the motion of plane matter. For example, if water flows down into a central sink placed near its (horizontal) surface, then air (which is above water) is entrained and forms a jet flow, which corresponds to the Squire solution far from the sink. Such an interpretation means, as follows from the solution, that at some finite strength of the sink, the jet momentum becomes infinite and the regular solution loses existence. This feature is conserved under generalization to swirling flows bounded by a conical surface, as follows from results of Goldshtik (1981), and Yih *et al.* (1982), together with the appropriate interpretation. In this work the solution existence bound is calculated and improved analytical estimates for it are obtained. The limit transition when the cone angle tends to zero is analysed too. Some speculations are presented concerning possible application of these solutions to model a driving mechanism of recently observed astrophysical jets (Lada 1985).

One may find additional information on the conically similar solutions in Goldshtik (1981), Pillow & Paull (1985) and Paull & Pillow (1985*a*, *b*). The existence loss due to flow collapse has also been found in MHD problems (Sozou 1971; Boyarevich *et al.* 1985). Obviously, a real flow must change before the singularity occurs, most likely becoming turbulent. This may cause another interesting phenomenon – a bifurcation of self-swirling regimes (Goldshtik & Shtern 1988). A number of results on conical viscous flows are reported in the monograph by Goldshtik, Shtern & Yavorsky (1989).

Here only the laminar steady axisymmetrical regimes are studied. The governing system of ordinary differential equations is derived and the applied boundary conditions are formulated in §2. A possibility of singularity appearance and its consequences are considered in §3. In §4 the inner and outer asymptotic expansions for near-critical solutions are constructed, and analytical estimates are made for solution existence boundaries in a parameter space. The numerical calculation results of these boundaries, some limit transitions, and velocity distributions are reported in §5. Moreover, solution non-uniqueness in the Serrin problem is shown. Ways of overcoming the paradox and possible applications are discussed in §6. In the conclusion (§7) the main results are summarized.

2. Problem formulation

We shall consider here steady solutions of the Navier–Stokes equations having the representation

$$\left.\begin{aligned} v_r &= -\frac{\nu}{r}y'(x), \quad v_\theta = -\frac{\nu}{r}\frac{y(x)}{\sin\theta}, \quad v_\varphi = \frac{\nu\Gamma(x)}{r\sin\theta}, \\ p &= \frac{\rho\nu^2}{r^2}q(x), \qquad x = \cos\theta. \end{aligned}\right\} \tag{2.1}$$

Here (r,θ,φ) are spherical coordinates; r is the distance from the origin; θ is the angle between the radius vector and the positive z-axis; φ is the angle about the z-axis; v_r, v_θ, v_φ and p are the velocity components and pressure; y, q, Γ are dimensionless functions; the prime denotes differentiation with respect to x.

Substituting (2.1) in the Navier–Stokes equations, we obtain after some simple transformations the system of ordinary differential equations

$$(1-x^2)\,\Gamma'' = y\Gamma', \tag{2.2}$$

$$(1-x^2)^2\,y^{\mathrm{IV}} - 4x(1-x^2)\,y''' = 2\Gamma\Gamma' + \tfrac{1}{2}(1-x^2)\,(y^2)'''. \tag{2.3}$$

When their solution is found, the pressure is determined with the help of the expression

$$q = \tfrac{1}{2}(1-x^2)\,y''' - xy'' - \tfrac{1}{4}(y^2)' - \frac{y^2+\Gamma^2}{2(1-x^2)}. \tag{2.4}$$

It is convenient to introduce a function $F(x)$ satisfying

$$F''' = 2\Gamma\Gamma'(1-x^2)^{-1} \tag{2.5}$$

with some relevant boundary conditions. Then after division by $(1-x^2)$ equation (2.3) may be integrated three times, with the result

$$(1-x^2)\,y' + 2xy - \tfrac{1}{2}y^2 = F(x). \tag{2.6}$$

Using the transformation

$$y = -2(1-x^2)\,U'/U \tag{2.7}$$

we find from (2.6) that

$$U'' + F(x)[2(1-x^2)^2]^{-1}\,U = 0. \tag{2.8}$$

Now boundary conditions are to be formulated. A pair from the following boundaries (W, FA, CVB, VL) will be used.

W denotes a rigid conical wall at $x = x_{\mathrm{w}}$. The adherence conditions to be fulfilled there are

$$y(x_{\mathrm{w}}) = y'(x_{\mathrm{w}}) = \Gamma(x_{\mathrm{w}}) = 0. \tag{2.9}$$

FA denotes a free half-axis at $x = -1$. There the regularity demands are

$$y(-1) = \Gamma(-1) = 0, \quad |y'(-1)| < \infty. \tag{2.10}$$

CVB denotes a conical vortex boundary at $x = x_{\mathrm{c}}$. There we shall use the conditions

$$y(x_{\mathrm{c}}) = 0, \quad \Gamma(x_{\mathrm{c}}) = \Gamma_1, \quad (1-x_{\mathrm{c}})\,y''(x_{\mathrm{c}}) = -A. \tag{2.11}$$

The first condition (impermeability) means that the boundary consists of streamlines, so that the normal velocity component equals zero. The second

condition defines the azimuthal velocity value, and the third condition defines the surface radial friction. Indeed, for this component of the stress tensor we have

$$\tau_{r\theta} = \rho\nu\left(r\frac{\partial}{\partial r}\frac{v_\theta}{r}+\frac{1}{r}\frac{\partial v_r}{\partial\theta}\right) = \frac{\rho\nu^2}{r^2\sin\theta}[(1-x^2)\,y''+2y].$$

Multiplying $-\tau_{r\theta}$ by $r\sin\theta\cos\theta$ and integrating with respect to φ, we produce the axial component of the friction force per unit length of the symmetry axis, which drives the radial fluid motion,

$$F_z = 2\pi x_c(1+x_c)\,A\rho\nu^2 r^{-1}.$$

Thus, the independent parameters Γ_1 and A are characteristics of fluid motion sources acting at the cone surface $x = x_c$.

VL denotes a vortex half-line placed at $x = 1$. It may be considered as the limiting case of CVB, when $x_c \to 1$ but the Γ_1 and A values are conserved. In this case, $y(x)$ has the representation, near $x = 1$,

$$y = -At\log t[1+o(1)],\quad t = 1-x,$$
$$y' = A\log t[1+o(1)],\quad y'' = -At^{-1}[1+o(1)],$$

where $o(1)$ means any continuous function of t, satisfying the condition $o(1)\to 0$ when $t\to 0$. Therefore, the boundary conditions at the vortex line are (Serrin 1972)

$$y(1) = 0,\quad \Gamma(1) = \Gamma_1,\quad \lim_{x\to 1}(1-x)\,y''(x) = -A. \tag{2.12}$$

If $A \neq 0$, then along the axis, fluid is driven by the force

$$F_z = 4\pi A\rho\nu^2 r^{-1} \tag{2.13}$$

acting per unit length of the axis.

In formulating conditions (2.12), Serrin used different parameters:

$$k = \tfrac{1}{2}\Gamma_1,\quad P = 1+4A\Gamma_1^{-2}. \tag{2.14}$$

The case $A = 0$ studied by Goldshtik (1960) allows a simple physical interpretation. One may think of the motion as driven by rotation of a thin rigid cylinder (a needle). When $A \neq 0$, the vortex half-line (and a conical vortex too) may be considered as a (turbulent) core of an atmospheric tornado (Serrin 1972). The vertical motion of the tornado core may be caused by the buoyancy force, for example.

The conditions for Γ_1 and y induce the consequent conditions for F, by using (1.6) and its first derivative, namely

$$(1-x^2)\,y''+2y-yy' = F'(x); \tag{2.15}$$

in particular, in case VL we have

$$F(1) = 0,\quad F'(1) = -2A. \tag{2.16}$$

3. Possibility of loss of solution existence

It is necessary for the existence of a regular solution $y(x)$ that function $U(x)$ has no zeros in the interval of x being considered. Indeed, as follows from (2.7), a zero of $U(x)$ means a pole of $y(x)$. In the case of a slow (creeping) motion the solution obviously exists. But with motion intensity increase, a pole $x = x_p$ of function $y(x)$ may

approach the interval and penetrate into it, passing through $x = -1$ or $x = 1$ (Goldshtik 1960). Let, for instance, the problem interval be $[x_w, 1]$. Here we shall consider $F(x)$ as an arbitrary continuous function satisfying conditions (2.16). Then $U(x)$ may be found as a solution of the initial-value problem by integration of (2.8) using the conditions

$$U(x_w) = 1, \quad U'(x_w) = 0. \tag{3.1}$$

The first condition (normalization) is formulated without any loss of generality, as according to (2.7) $U(x)$ is determined up to an arbitrary numerical factor. The second condition (3.1) follows from (2.7) and (2.9). When $F \equiv 0$, which is correct at $\Gamma_1 = A = 0$, we have $U \equiv 1$. Owing to continuity, if $|\Gamma_1|$ and $|A|$ are small enough, then x_p is placed (if it exists) far from the interval $[x_w, 1]$. Zeros of $U(x)$ cannot be generated inside the interval owing to a tangent bifurcation. Suppose the tangent situation takes place at point $x = x_p$. Then $U(x_p) = U'(x_p) = 0$, and from (2.8) it follows that $U \equiv 0$, which contradicts (3.1). Thus, a zero of $U(x)$ may penetrate into the interval only by passing through $x = 1$. To know what happens in this case, let us study solution features near $x = 1$. According to conditions (2.16), $F(x)$ has the structure

$$F = 2At\,[1 + o(1)],$$

and therefore equation (2.8) may be rewritten in the form

$$U'' + A(4t)^{-1}[1 + o(1)]\,U = 0.$$

Its general solution has at small t the representation $U = B_1 U_1 + B_2 U_2$, where $U_1 = t - \frac{1}{8}At^2\ [1 + o(1)]$, $U_2 = 1 - \frac{1}{4}At(\ln t - 1) + t \cdot o(1)$. When a zero of $U(x)$ passes through $x = 1$, the value of B_2, being a function of parameters Γ_1 and A, becomes zero. Hence at $x_p = 1$ we have $U = B_1 U_1$ and according to (2.7)

$$y = 2(1 + x) + o(1). \tag{3.2}$$

Thus, in the critical situation the zero $x = 1$ and the pole $x = x_p$ of function $y(x)$ merge, and $y(x)$ has the finite value $y(1) = 4$. As at subcritical parameter values $y(1) = 0$, the existence loss is preceded by the generation of a boundary layer. This layer corresponds to a strong upward jet. The jet attracts ambient fluid and in the limit a sink is formed at the axis. The sink strength is independent of parameter values and equals $8\pi\nu$ per unit length of the axis. (If the pole $x = x_p$ passes through $x = -1$, then at $x_p = -1$ one has $y(-1) = -4$.)

Such a singularity appears in the Squire solution at the free axis, in the needle–wall interaction problem (Goldshtik 1960) and in the Serrin (1972) problem at the line vortex, as will be shown below. Though the initial boundary conditions are different in these problems the possible additional singularity at the axis is the same, and it is the sink. The appearance of the sink means loss of existence of the initial problem solution. If the flow region does not contain the symmetry axis, being bounded by two cones, then the singularity may not occur at any finite parameter values (Goldshtik & Shtern 1987).

To find the parameter values at which the singularity occurs, it is convenient to use the asymptotic expansion method.

4. Asymptotic analysis

4.1. *Inner expansion*

First, we consider $A = 0$. In this case $y'(1)$ is bounded in the subcritical situation, but when x_p decreases and approaches 1 then $y'(1) \to -\infty$. Introducing the small

parameter $\epsilon = -1/y'(1)$ and the boundary-layer variable $\eta = (1-x)/\epsilon$, we use them in (2.6) with $\epsilon \to 0$. The right-hand side limit is zero from conditions (2.16). Then equation (2.6) is decoupled from the whole system in the boundary-layer approximation and takes the form

$$\eta y_i' = y_i - \tfrac{1}{4}y_i^2, \quad y_i(0) = 0,$$

where y_i is the leading term of the inner expansion of y, and the prime denotes differentiation with respect to η. Its solution is

$$y_i = 4\eta/(4+\eta). \tag{4.1}$$

This coincides with the Schlichting (1965) self-similar solution for a submerged round jet. As $\eta \to \infty$ one has $y_i \to 4$, in accordance with the result of §3. Similar transformation of (1.2) together with (4.1) yields

$$\Gamma_i'' = -2\Gamma_i'/(4+\eta), \quad \Gamma_i(0) = \Gamma_1, \quad |\Gamma_i(\infty)| < \infty.$$

Its solution $\Gamma_i = 4\Gamma_1/(4+\eta)$ coincides with the solution found by Zubtsov (1984).

In the case of $A \neq 0$, the value $y'(1)$ is infinite at subcritical parameter values too. Hence, the small parameter must be chosen in a different way, for instance $\epsilon = x_p - 1$. Nonetheless, the leading terms of the asymptotic expansion y_i, Γ_i preserve their form, and the logarithmic singularity is reflected in the following terms.

The Schlichting solution (4.1) serves as the universal asymptotic part for all cases of singularity appearance in the conical class, i.e. for swirling or non-swirling flows, for the free axis (FA) and the vortex half-line (VL). In the free-axis case, the circulation is $\Gamma_i = \frac{1}{4}\Gamma_1 y_i = \Gamma_1 \eta/(4+\eta)$. This result may be checked explicitly.

Naturally, the outer expansion is not universal and each case must be considered separately.

4.2. *Outer expansion in the case of the free axis*

The problem of the free conical vortex is formulated in the region $-1 \leqslant x \leqslant x_c$ using boundary conditions (2.10), (2.11). From (2.6), (2.7) we obtain the conditions for $F(x)$ as

$$F(-1) = F'(-1) = 0, \quad F'(x_c) = -(1+x_c)A.$$

Then from (2.5), with the help of easy but rather bulky transformations, we have

$$F(x) = \frac{2x_c x - 1 - x^2}{2(1+x_c)} \int_{-1}^{x} \frac{\Gamma^2 - \Gamma_1^2}{(1-t)^2}\,dt - \frac{(1+x)^2}{(1+x_c)^2} \int_{x}^{x_c} \frac{x_c - t}{1-t^2}\,\Gamma\Gamma'\,dt$$

$$-\tfrac{1}{4}\Gamma_1^2 \frac{1+x}{1+x_c}(1-x+2x_c) - \tfrac{1}{2}A(1+x)^2 - \frac{(x_c-x)(1+x)(\Gamma^2-\Gamma_1^2)}{2(1+x_c)(1-x)}. \tag{4.2}$$

One may check (4.2) by direct differentiation. The main part of the outer expansion for the circulation is trivial: $\Gamma_o(x) \equiv \Gamma_1$. Indeed, it satisfies equation (2.2) and condition (2.11). Further, it follows from (2.2) that

$$\Gamma'(x) = \Gamma'(x_c) \exp\left\{ -\int_x^{x_c} y(t)\,(1-t^2)^{-1}\,dt \right\}.$$

In the critical situation, when $y(-1) = -4$ and the integral becomes singular, one must have $\Gamma'(x_c) = 0$ and therefore $\Gamma'(x) \equiv 0$. Substituting $\Gamma \equiv \Gamma_1$ in (4.2), we produce the outer form for $F(x)$,

$$F_o(x) = -\tfrac{1}{4}\Gamma_1^2 \frac{1+x}{1+x_c}(1-x+2x_c) - \tfrac{1}{2}A(1+x)^2.$$

The equation for the leading term of the outer expansion, $y_0(x)$, coincides with (2.6) after replacing F by F_0. Introducing U_0, similar to (2.7), we reduce the problem to the linear one

$$U_0'' - \frac{\Gamma_1^2(1-x+2x_c)+2A(1+x_c)(1+x)}{8(1+x_c)(1+x)(1-x)^2}U_0 = 0, \tag{4.3}$$

$$U_0(x_c) = 1, \quad U_0'(x_c) = 0, \quad U_0(-1) = 0.$$

The equation and the first two conditions may be considered as an initial-value problem. The third condition gives the relation between Γ_1 and A at the solution existence boundary.

If $A \geqslant -\Gamma_1^2\,[2(1+x_c)]^{-1}$, then $F_0(x) \leqslant 0$, $U'' \geqslant 0$ in the integration interval, so that the condition $U_0(-1) = 0$ may not be fulfilled. Therefore existence loss is possible only when the force acting on fluid from the cone surface is directed towards the origin and is large enough.

If $A < -\Gamma_1^2[2(1+x_c)]^{-1}$, then $F_0(x)$ changes its sign inside the interval $(-1, x_c)$ at $x = x_0$, where

$$x_0 = -1+2\frac{1+x_c}{1+s}, \quad s = -2A\Gamma_1^{-2}(1+x_c). \tag{4.4}$$

When s runs from 1 to ∞, x_0 varies from x_c to -1. In this case, it is useful to rewrite (4.3) in the more compact form

$$U_0'' = -\frac{b(x-x_0)}{(1+x)(1-x)^2}U_0, \quad b = \frac{\Gamma_1^2(1+s)}{8(1+x_c)}, \tag{4.5}$$

and as the integral equation

$$U_0(x) = 1+b\int_x^{x_c}\frac{(x-t)(t-x_0)}{(1+t)(1-t)^2}U_0(t)\,\mathrm{d}t. \tag{4.6}$$

At the critical parameter values, $U_0(-1) = 0$, $U_0(x_0) > 0$. In the interval (x_0, x_c), the function $U_0(x)$ increases monotonically and $U_0''(x) \leqslant 0$, so there are bounds

$$\frac{x-x_0}{x_c-x_0} \leqslant U_0(x) \leqslant 1.$$

Substituting $x = x_0$ in (4.6) we have

$$0 \leqslant U_0(x_0) = 1-b\int_{x_0}^{x_c}\frac{(t-x_0)^2\,U_0(t)}{(1+t)(1-t)^2}\,\mathrm{d}t,$$

from which

$$\frac{1}{b} \geqslant \int_{x_0}^{x_c}\frac{(t-x_0)^2\,U_0(t)}{(1+t)(1-t)^2}\,\mathrm{d}t \geqslant \int_{x_0}^{x_c}\frac{(t-x_0)^3\,\mathrm{d}t}{(1+t)(1-t)^2\,(x_c-x_0)}.$$

Calculating the integral we obtain the estimate

$$b \leqslant b_u = \left\{1+\frac{(1-x_0)^2}{2(1-x_c)}+B_2\log\frac{1-x_0}{1-x_c}-B_1\log\frac{1+x_c}{1+x_0}\right\}^{-1}, \tag{4.7}$$

where

$$B_1 = \frac{(1+x_0)^3}{4(x_c-x_0)}, \quad B_2 = \frac{3x_0-1}{x_c-x_0}-B_1.$$

On the other hand, using $x = -1$ in (4.6) we have

$$0 = 1 + b\int_{-1}^{x_0} \frac{x_0 - t}{(1-t)^2} U_0(t)\,\mathrm{d}t - b\int_{x_0}^{x_c} \frac{t - x_0}{(1-t)^2} U_0(t)\,\mathrm{d}t$$

$$\geqslant 1 - b\int_{x_0}^{x_c} \frac{t - x_0}{(1-t)^2}\,\mathrm{d}t.$$

For the latter inequality we use $U_0 \geqslant 0$ for $-1 \leqslant x \leqslant x_0$ and $U_0 \leqslant 1$ for $x_0 \leqslant x \leqslant x_c$. As a result, we find the lower bound

$$b \geqslant b_\ell = (1-x_c)\left\{(1+x_c)\frac{s-1}{s+1} + (1-x_c)\log\frac{(1-x_c)(1+s)}{2(s-x_c)}\right\}^{-1}. \tag{4.8}$$

Formulae (4.7), (4.8), taking into account notations (4.4), (4.5), accordingly give the upper and the lower $(-A)$ values at fixed Γ_1. In the limit $x_c \to 1$ both estimates coincide and take the form

$$A = -\tfrac{1}{4}\Gamma_1^2. \tag{4.9}$$

When $\Gamma_1 \gg 1$ the linear terms on the left of (2.6) may be neglected and then we have

$$y_0^2 \approx 4b(x_0 - x)(1+x).$$

The right-hand expression must be positive in the flow core, and so it follows that $x_0 \to x_c$ when $\Gamma_1 \to \infty$. Equation (4.4) yields $s \to 1$, so that the asymptotic relation at the existence boundary is

$$A = -\Gamma_1^2[2(1+x_c)]^{-1}. \tag{4.10}$$

This relation is in accordance with (4.9) and it reduces to (4.9) at $x_c = 1$.

The flow structure in the near-critical case when $\Gamma_1 \gg 1$ includes the axial boundary layer (the Schlichting jet) with arbitrarily large velocity values, the potential core with velocities proportional to Γ_1, and a viscous layer near the cone with a thickness $\sim \Gamma_1^{-\frac{2}{3}}$ in which the radial velocity increases to a value $\sim \Gamma_1^{\frac{4}{3}}$ (Goldshtik & Shtern 1987).

4.3. *Outer expansion in the case of the vortex line*

The problem of the interaction between the vortex half-line and the conical wall is considered in the region $x_w \leqslant x < 1$, using boundary conditions (2.9), (2.12). According to (2.6), at the wall $F(x_w) = 0$, and $F(x)$ has to satisfy conditions (2.16) at the vortex line. Then from (2.5), following Goldshtik (1960) and Serrin (1972), we have after some transformations

$$F(x) = C(x - x_w)(1-x) - (1-x)^2\int_{x_w}^{1} \frac{t\Gamma^2}{(1-t^2)^2}\,\mathrm{d}t$$

$$+ x_w\frac{1-x}{1-x_w}\int_{x_w}^{x} \frac{\Gamma^2}{(1+t)^2}\,\mathrm{d}t - \frac{x - x_w}{1-x_w}\int_{x}^{1} \frac{\Gamma^2}{(1+t)^2}\,\mathrm{d}t, \tag{4.11}$$

where

$$C = \frac{\Gamma_1^2 + 4A}{2(1-x_w)} - \frac{x_w}{(1-x_w)^2}\int_{x_w}^{1} \frac{\Gamma^2}{(1+t)^2}\,\mathrm{d}t.$$

One may check that $F(x)$ defined by (4.11) satisfies (2.6) and the boundary conditions. The equation (2.2) may be transformed to the integral form

$$\Gamma = \Gamma_1 \phi(x)/\phi(1), \quad \phi(x) = \int_{x_w}^{x} \exp\left\{\int_{x_w}^{t} z\,\mathrm{d}u\right\}\mathrm{d}t,$$

$$z = y/(1-x^2).$$

Because $y(1) = 4$ in the critical situation, function $z(x)$ has, owing to (3.2), the structure

$$z = 2(1-x)^{-1} + f(x),$$

where $(1-x)f(x)$ tends to zero when $x \to 1$. Therefore, we have

$$\exp\left\{\int_{x_w}^{t} z\,\mathrm{d}u\right\} = \left(\frac{1-x_w}{1-t}\right)^2 \exp\left\{\int_{x_w}^{t} f(u)\,\mathrm{d}u\right\}.$$

Because the singularity is strong enough, $\phi(1)$ is infinitely large. But for $x < 1$, $\phi(x)$ is bounded, hence $\Gamma \equiv 0$ in the interval $x_w \leqslant x < 1$. This result is in accordance with the asymptotic analysis. Indeed, the inner expansion solution $\Gamma_1 = 4\Gamma_1/(4+\eta)$ tends to zero as $\eta \to \infty$. The theory of asymptotic expansion matching (Van Dyke 1975) demands that the outer approximation of the inner solution coincides with the inner approximation of the outer solution. This implies that $\Gamma_0(1) = 0$. Then from (2.2) and (2.9) it follows that $\Gamma_0 \equiv 0$. Using the result of (4.11), we find the outer form of $F(x)$,

$$F_0(x) = C(x-x_w)(1-x), \quad C = (\Gamma_1^2 + 4A)[2(1-x_w)]^{-1}. \tag{4.12}$$

Thus $y_0(x)$, the leading term of the outer expansion, must be found as a solution of the problem

$$\left.\begin{aligned} (1-x^2)\,y_0' + 2xy_0 - \tfrac{1}{2}y_0^2 &= C(x-x_w)(1-x), \\ y_0(x_w) = 0, \quad y_0(1) = 4, \quad y_0'(1) &= 2 - \tfrac{1}{4}(1-x_w)\,C. \end{aligned}\right\} \tag{4.13}$$

The latter condition follows from (4.13) after differentiation and substitution of $x = 1, y_0 = 4$. Equation (4.13) has to be integrated as an initial-value problem from $x = 1$ to $x = x_w$, and constant C must be chosen so that $y(x_w) = 0$.

The problem (4.13) was considered by Serrin (1972), Goldshtik (1981) and Schneider (1981), but in different contexts. Schneider used the solution of (4.13) to describe an outer flow induced by a strong jet emerging from a hole in a wall. A self-similar solution of this problem does not exist. But when the jet momentum is high enough, the asymptotic expansions approximate satisfactorily the real rather complex flow structure (Schneider, Zauner & Bohm 1987). In our case, equation (4.13) provides the outer expansion of the exact solution of the Navier–Stokes equations.

The upper and the lower bounds of $C(x_w)$ may be found analytically. Again, with the help of transformation (2.7) it is convenient to reduce the problem to the linear one,

$$U_0'' + \frac{C(x-x_w)}{2(1-x)(1+x)^2}\,U_0 = 0. \tag{4.14}$$

Constant C must be found as the first eigenvalue of equation (4.14) under the conditions $U_0'(x_w) = 0$, $U_0(1) = 0$. Using the normalization $U_0(x_w) = 1$ we reduce the problem to the integral equation

$$U_0(x) = 1 - \tfrac{1}{2}C\int_{x_w}^{x} \frac{(x-t)(t-x_w)}{(1-t)(1+t)^2}\,U_0(t)\,\mathrm{d}t. \tag{4.15}$$

Putting $x = 1$ we find

$$\frac{2}{C} = \int_{x_w}^{1} \frac{t - x_w}{(1+t)^2} U_0(t)\, dt. \tag{4.16}$$

As it is supposed that $x = 1$ is the first zero of $U(x)$ at $x \geqslant x_w$, we have $U_0(x) \geqslant 0$ for $x_w \leqslant x < 1$. It yields $C \geqslant 0$ from (4.16) and $U_0''(x) \leqslant 0$ from (4.14). Then $U_0'(x) \leqslant 0$ on $(x_w, 1)$, as $U_0'(x_w) = 0$. On the other hand, $U_0(x) \leqslant 1$ from (4.15). Thus $U_0(x)$ has bounds

$$(1-x)/(1-x_w) \leqslant U_0(x) \leqslant 1.$$

Using these bounds in (4.16) we obtain $C_\ell \leqslant C \leqslant C_u$, where

$$C_\ell = 4\left\{2\log\frac{2}{1+x_w} - 1 + x_w\right\}^{-1}, \quad C_u = \left\{\frac{3+x_w}{2(1-x_w)}\log\frac{2}{1+x_w} - 1\right\}^{-1}. \tag{4.17}$$

The asymptotic forms of (4.17) are $C_u = 4C_\ell = 48(1-x_w)^{-2}$ as $x_w \to 1$ and $C_\ell = C = C_u = (\frac{1}{2}\log(2/(1+x_w)))^{-1}$ as $x_w \to -1$. When function $C(x_w)$ is found (it will be calculated further) the equation for the boundary of the solution existence region in the parameter space has the form

$$\Gamma_1^2 + 4A = 2(1-x_w)\, C(x_w). \tag{4.18}$$

In the limit $x_w \to -1$ we have the problem of the vortex half-line in a free space. So as $C(-1) = 0$, equation (4.18) is reduced to $\Gamma_1^2 + 4A = 0$ which formally coincides with (4.9), but the formulae have different meanings. Relation (4.18) means that the solution does not exist for $\Gamma_1^2 + 4A > 0$ owing to a sink singularity at $x = 1$, whereas relation (4.9) means that the solution does not exist at $\Gamma_1^2 + 4A < 0$ owing to the singularity at $x = -1$.

The unique possibility for solution existence is that $\Gamma_1^2 + 4A = 0$ must be fulfilled. It can be shown (Goldshtik 1981) that in this case the regular solution not only exists but moreover is a function of two independent parameters – say, the circulation Γ_1 and an axial flux of the kinematic momentum J. Both the parameters may vary from $-\infty$ to ∞. Parameter A is not independent, as $A = -\frac{1}{4}\Gamma_1^2$. The solution $y_0(x) = 2(1+x)$ of (4.13) at $x_w = -1$ ($C = 0$) is the limit of the problem of the free vortex half-line when $J \to \infty$.

5. Numerical results

5.1. *Interaction between a rotating needle and a plane wall*

The problem is considered in the region $x_w = 0 \leqslant x \leqslant 1$. The system of equations (2.2), (2.5), (2.6) with boundary conditions (2.9), (2.12) is calculated by the following algorithm. At $x = 0$ condition (2.9) is supplemented by $\Gamma'(0) = a$, $F'(0) = C_2$, $F''(0) = -C_1$ where a, C_1, C_2 are supported by some tentative values. Further, $F(0) = 0$ follows from (2.9). So we have the initial-value problem, which is integrated from $x = 0$ to $x = 1$. After integration we want conditions (2.16) with $A = 0$ to be satisfied. To this end, two of the three parameters a, C_1, C_2 must be chosen in a special way. As a rule, a and C_2 have been found by shooting. Parameter C_1 remains free and determines implicitly $\Gamma(1) = \Gamma_1$. The value of Γ_1 depends on C_1 monotonically. The critical value of $\Gamma_1 = \Gamma_*$ is found by solving (4.13). For $x_w = A = 0$ we obtain $C = C_{1*} = 15.2894$, $\Gamma_* = (2C)^{\frac{1}{2}} = 5.5298$ (see (4.12)).

The solution structure at $\Gamma_1 = 5.473$ is shown in figure 1. This Γ_1 value corresponds to $y(1) = -460.5$ (according to Schlichting 1965, in a turbulent round jet the eddy

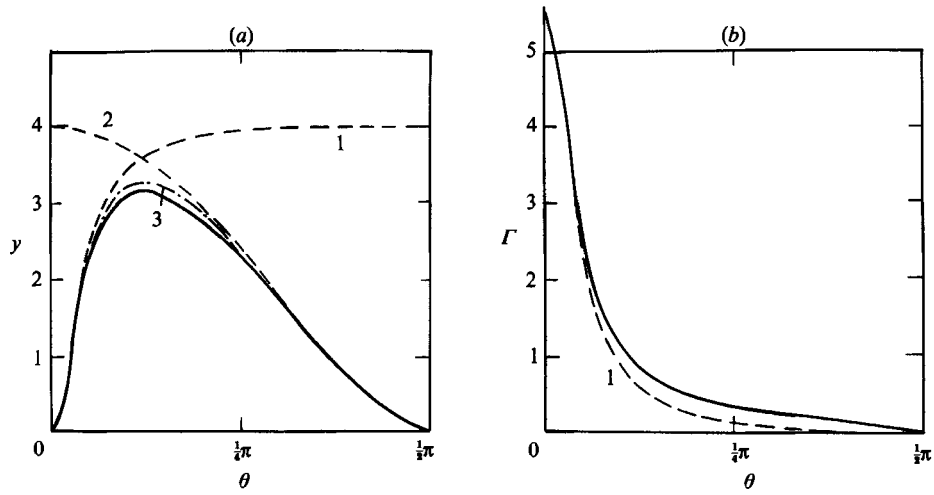

FIGURE 1. Distribution of (*a*) the dimensionless stream functions of the meridional motion (*b*) the circulation for a near-critical regime for the problem of rotating needle–wall interaction. 1, inner; 2, outer; 3, uniform asymptotic expansions.

viscosity ν_t is produced so that $rv_r/\nu_t \approx 460.5$). For comparison the inner solutions y_i, Γ_i (see §4.1), the outer solution $y_o(x)$ (which is the solution of (4.13) at $C = C_{1*}$) and the uniform asymptotic approximation $y_u(x) = y_o(x) + y_i(x) - 4$ used by Schneider, are also shown. Contrary to the case of the Schneider problem, y_u may here be compared with the exact solution.

Parameters a and C_2 are related to the wall shear stress though $\tau_{\theta\varphi} = -a\rho\nu^2 r^{-2}$, $\tau_{r\theta} = C_2\rho\nu^2 r^{-2}$.

Values of a and C_2 as functions Γ_1 are shown in figure 2. The azimuthal friction first increases with Γ_1, but then decreases and returns to zero at $\Gamma_1 = \Gamma_*$. It means that the rotating fluid motion ceases outside the vortex line. The results indicate that an interesting physical effect may be predicted. If one were to rotate a thin rigid cylinder which is normal to a wall, then at small angular velocities the cylinder causes a swirl of the ambient fluid. But when the velocity becomes large enough, rotation decreases far from the cylinder and finally vanishes everywhere apart from a small region near the cylinder. Let us study this effect in more detail, replacing the vortex half-line by a conical vortex with a small angle.

5.2. *Interaction of a conical vortex with a plane wall*

This problem is considered in the region $x_w = 0 \leqslant x \leqslant x_c < 1$. We seek the solution of system (2.2), (2.5), (2.6) under boundary conditions (2.9), (2.11). The algorithm is the same as in §5.1, with the difference that integration runs up to x_c, where the outer conditions are satisfied. Here two cases are studied: (*a*) An adherence condition for the meridional motion, $y'(x_c) = 0$. This corresponds to a special choice of A in (2.11). (*b*) The absence of radial friction, i.e. $y''(x_c) = 0$. This corresponds to $A = 0$ in (2.11).

In both of these cases the condition $y(x_c) = 0$ must be satisfied too. Some calculated results are shown in figure 2. The numerical results indicate that if $x_c < 1$, then solutions exist for all Γ_1 values. At $\Gamma_1 < \Gamma_*$ when $x_c \to 1$, the solutions tend uniformly to the solution at $x_c = 1$. When $\Gamma_1 \geqslant \Gamma_*$ we find that $a \to 0$, $C_2 \to C_{1*}$ as $x_c \to 1$. Consequently, the functions $y(x)$, $\Gamma(x)$ tend to $y_o(x)$ and zero. The transition dynamics for the y- and Γ-distributions are shown in figure 3 for $\Gamma_1 = 20$. The

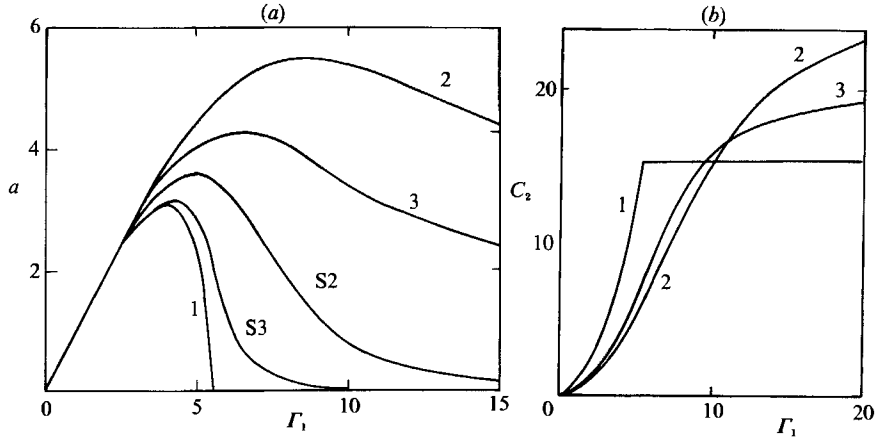

FIGURE 2. Dependence of (*a*) azimuthal and (*b*) radial wall friction on the circulation for the cases of 1, the needle and cones under the condition $v_r = 0$ (2, $x_c = 0.99$; 3, 0.999) and the condition $\partial v_r/\partial\theta = 0$ (S2, $x_c = 0.99$; S3, 0.999).

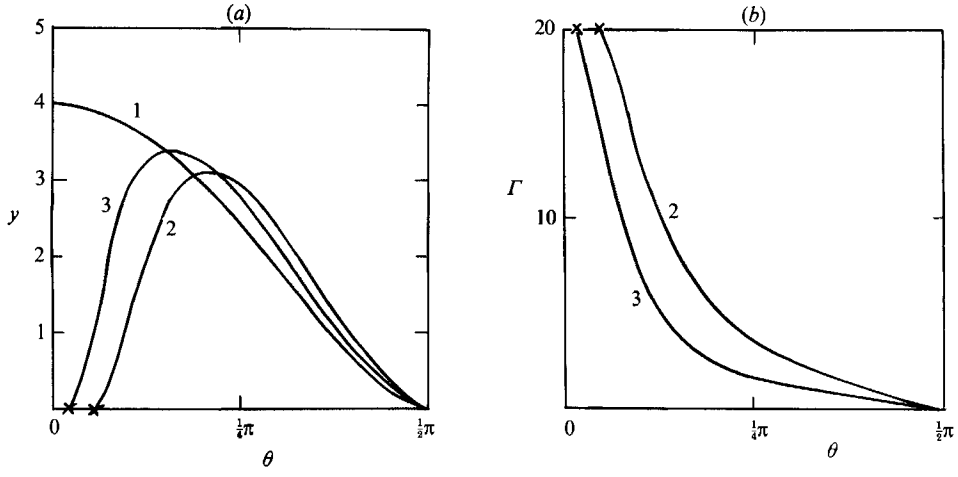

FIGURE 3. Distributions for the condition $v_r = 0$ at different cone angles. 1, $x_c = 1$; 2, 0.99; 3, 0.999.

solutions approach the limit distributions rather slowly; $y(x)$ at $x_c = 0.999$ differs appreciably from $y_0(x)$ (curve 1). But the result of the limit transition seems obvious. The limit regime becomes independent of the Γ_1 value and coincides with the limit, when $\Gamma \to \Gamma_*$ at $x_c = 1$. These results support the predicted effect of the rotating needle and the wall interaction.

In both formulations of the boundary conditions, when $x_c \to 1$ then $A \to 0$. But if we consider the transition $x_c \to 1$ with $A = \text{Const}$, then in the limit we obtain the Serrin problem.

5.3. *Solution non-uniqueness in the Serrin problem*

Serrin mentioned that he was unable to prove uniqueness. For the case $A = 0$ the uniqueness theorem has been proved for the whole solution existence region, i.e. for $\Gamma_1 < \Gamma_*$ (Goldshtik 1981). But here we show with the help of numerical calculations that for $A < 0$ and for Γ_1 large enough, the Serrin solution is not unique.

We have already pointed out that if $A = 0$, then fluid is driven by a force acting

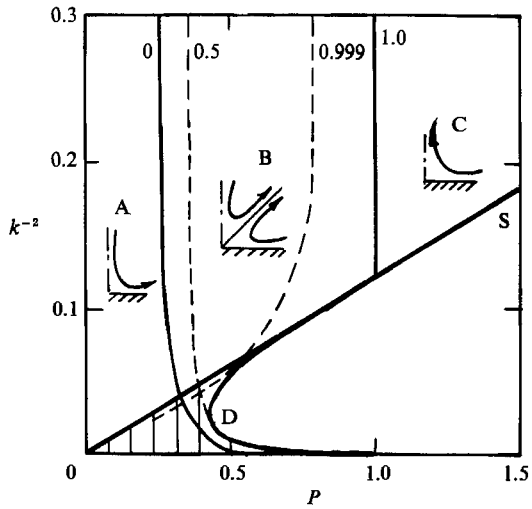

FIGURE 4. Regime map in the Serrin problem. Curves 0 and 1 separate subregions of downward (A), two-cell (B) and upward (C) flow regimes, S is the curve corresponding to sink appearance on the vortex line, D is the curve corresponding to two smooth solutions merging. Figures denote the x_s value for the respective curves (cone $x = x_s$ separates the cells).

along the symmetry axis, and its value per unit length is defined by (2.13). This force is an independent motion driver, and causes a flow even at $\Gamma_1 = 0$. The force may be considered as the mathematical model of a thin hot (upward) or cold (downward) jet in the near-axis region, which drives the ambient fluid. In the case of $x_w = \Gamma_1 = 0$, the singularity occurs, when A increases through the value $A = A_* = \frac{1}{2}C_{1*} = 7.6447$.

The regime map obtained numerically is shown in figure 4. For the sake of convenient comparison the Serrin parameters $k = \frac{1}{2}\Gamma_1$, $P = 1 + 4A\Gamma_1^{-2}$ are used. The numerical algorithm is similar to that in §5.1, but now it is sufficient to choose only one parameter from a, C_1, C_2 to satisfy $y(1) = 0$. The other two define, parametrically, values of Γ_1 and A.

According to Serrin, the existence region is placed to the left of the boundary which consists of the line S for $P > 1$ and the curve D for $P < 1$. The region was subdivided by Serrin into three subregions A, B, C, separated by curves 0 and 1 in figure 4. The subregions correspond to different structures of the meridional motion (see sketches in figure 4).

Our results agree with Serrin's, but provide some new information about the features of the problem. On the line S, which is the ray $k^{-2} = A_*^{-1}P$, the existence loss is caused by the appearance of the singularity. This mechanism has been studied in detail in the preceding part of the paper. But at curve D the existence loss has a different nature. In the hatched region of figure 4, two regular solutions exist for every k and P. At curve D these solutions, remaining regular, merge and disappear. One may think of subregion B as a sheet folded along line D, so that the dashed part is a continuation of B after folding.

Ray S for $P < 1$ is the left boundary of the dashed region. There the second solution loses its existence owing to the singularity. In the dashed part of B the solutions also have the two-cell structure. There are two dashed curves in figure 4 and each of them corresponds to a fixed value x_S, where $x = x_S$ is a cone separating the flow cells. Such curves are tangent to the boundary D, and at the tangent point they pass from one sheet of subregion B to another. If one moves in the dashed region to

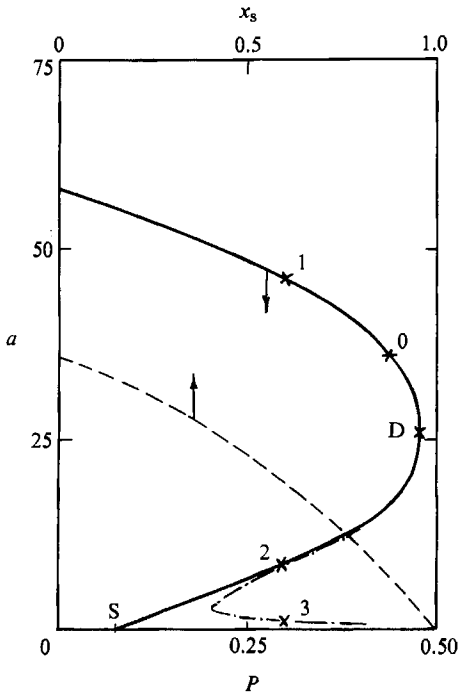

FIGURE 5. The azimuthal friction versus the axial force at $k = 10$. Points 0, D, S indicate intersections of the curve $k = \text{Const}$ with the same curves as those denoted similarly in figure 4. The dashed line shows the separating cone position. The dot-dash curve is the transformation of the solid one in the case of the vortex cone with $x_c = 0.999$.

ray S, keeping Γ_1 fixed, then x_S increases and achieves the value 1 at S. Lines S and D meet at the point $\Gamma_1 = \Gamma_*$, $P = 1$, where curve D terminates.

The correlation between a and P at a fixed circulation value $\Gamma_1 = 20$ ($k^{-2} = 0.01$) is shown in figure 5. A part of the upper branch on the left of the point 0 relates to subregion A in figure 4, segment OD relates to the first sheet of subregion B, and DS relates to the second one. In the interval $P_S < P < P_0$ the downward (upper branch) and two-cell (lower branch) regimes coexist. In the interval $P_0 < P < P_D$ a pair of two-cell solutions coexist. At $\Gamma_1 = 20$ we find $P_S = 0.08$, $P_0 = 0.44$, $P_D = 0.48$.

At point S of figure 5, a tends to zero and x_S becomes 1, and the sink singularity is formed on the symmetry axis. The latter may be avoided by changing the problem formulation. When the vortex cone $x = x_c = 0.999$ is used instead of the vortex line, the results are shown by the dot-dash curve in figure 5. The upper part of this curve is very close to the solid line. One sees a typical hysteresis phenomenon. An example of the velocity distributions for the coexisting solutions is illustrated in figure 6.

When Γ_1 increases, the $y(x)$ value remains finite where $y > 0$, and $|y|$ grows asymptotically proportional to Γ_1 where $y < 0$. For the two-cell solution in the interval $0 \leqslant x \leqslant x_S$ the problem may be considered separately as the interaction of the conical vortex $x_c = x_S$ and the wall $x_w = 0$. At high Γ_1 values, a strong conical jet near the cone $x = x_S$ develops and in the limit $\Gamma_1 \to \infty$ jumps in azimuthal and meridional velocities occur. The conical jet attracts a swirling fluid from the region near the axis and non-swirling fluid from the region near the wall. In as much as convection of momentum predominates over diffusion when $\Gamma_1 \gg 1$, the circulation is almost constant in the near-axis zone and rotation is practically absent in the near-

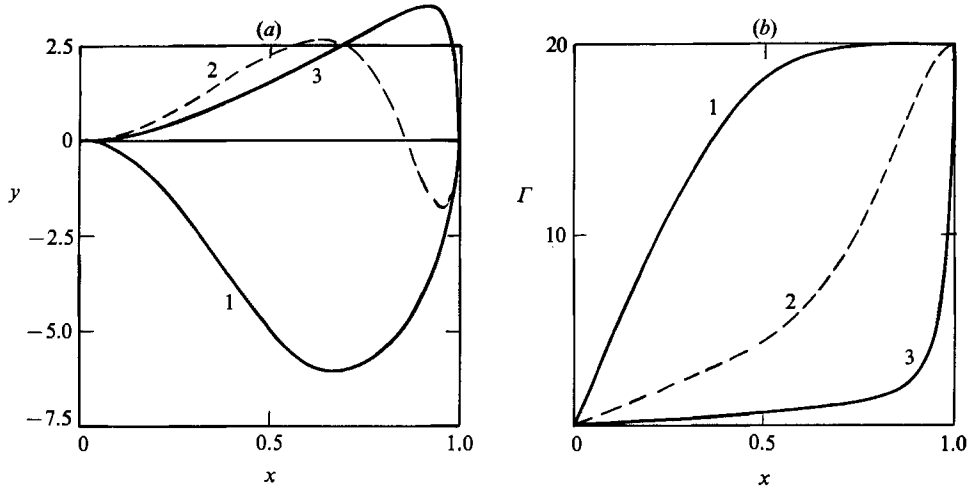

FIGURE 6. Distribution for the three coexisting solutions at $k = 10, P = 0.3$. 1, 2, 3 correspond to the points 1, 2, 3 in figure 5. The solid curves are used for stable regimes and the dashed curves for unstable ones.

wall zone. But if in the near-axis zone the flow has a potential limit when $\Gamma_1 \to \infty$, then in the near-wall zone the flow does not tend to a potential one, because the velocity remains finite there, and the influence of viscosity is maintained.

The potential limit in the whole region exists only for the downward regime. In this case it follows from (2.5) that $F''' = 0$, because $\Gamma(x) = \text{Const}$. Using boundary conditions (2.16) and $F(0) = 0$ we obtain $F(x) = 2Ax(1-x)$. Neglecting linear terms in the left-hand side of (2.6) we obtain the potential solution for $y(x)$:

$$y_p(x) = -2\{-Ax(1-x)\}^{\frac{1}{2}}. \tag{5.1}$$

Serrin (1972) has proved that the downward regimes exist for $A \leqslant -|k|(1+\log|k|)$. This inequality estimates from below the growth of $|y_p(x)|$ when $\Gamma_1 \to \infty$.

Solution (5.1) satisfies $y(1) = 0$, but $y_p'(x)$ has a stronger singularity at $x = 1$ than the logarithmic one. Besides, $y_p(x)$ satisfies the impermeability condition at the wall, but $y_p'(x)$ tends to infinity at $x = 0$. For $\Gamma_1 \gg 1$ it causes the development of near-axis and near-wall boundary layers. In the Serrin model the near-axis layer has no physical meaning. Let us consider the near-wall boundary layer.

For $\Gamma_1 \gg 1$, equation (2.6) takes the form

$$(1-x^2)y' + 2xy - \tfrac{1}{2}y^2 = 2Ax(1-x). \tag{5.2}$$

Introducing new variables

$$y = -(-2A)^{\frac{1}{3}}w, \quad \eta = (-2A)^{\frac{1}{3}}x$$

and letting $A \to \infty$, we obtain from (5.2)

$$\frac{dw}{d\eta} = \eta - \tfrac{1}{2}w^2, \quad w(0) = 0. \tag{5.3}$$

The solution of (5.3) may be explicitly expressed in terms of the Airy function, but it is simpler to find it numerically. The value of $dw/d\eta$ attains a maximum equal to 1.03 at $\eta = 1.5$ (curve 1 in figure 7). Thus, the boundary layer corresponds to a near-wall jet of width $\sim |A|^{-\frac{1}{3}}$ and the maximum velocity $\sim |A|^{\frac{2}{3}}$.

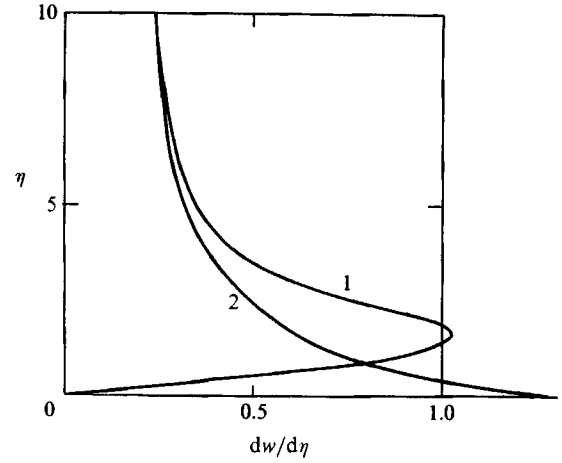

FIGURE 7. Radial velocity distribution in the near-plane boundary layer ($\Gamma_1 \gg 1$) for 1, the Serrin, and 2, the free-vortex problems.

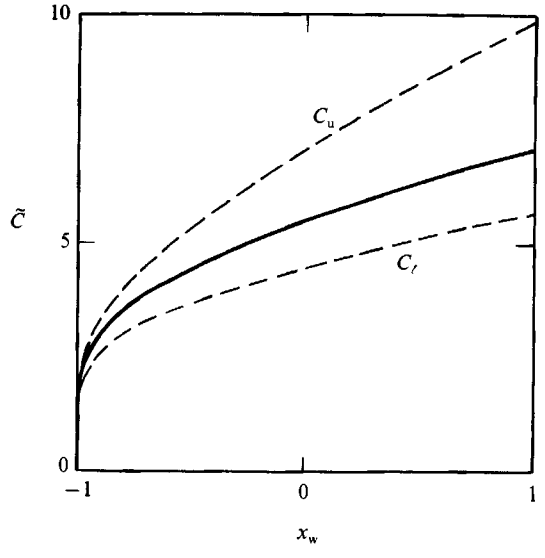

FIGURE 8. Critical value of the existence criterion versus the conical wall position in the generalized Serrin problem. The solid curve is found numerically, the dashed ones are analytical bounds (4.17). $\tilde{C} = [(1-x_w)(\Gamma_1^2+4A)]^{\frac{1}{2}}$.

When the wall is not the plane $x = 0$, but a cone, the regime map does not qualitatively change from the one shown in figure 4. In the typical case, ray S is defined by the equation

$$k^{-2} = 2P[(1-x_w)\,C(x_w)]^{-1},$$

where $C(x_w)$ is determined by solving the problem (4.13).

This relation has been found numerically and is shown in figure 8. For the sake of a compact graphical representation a new variable is used: $\tilde{C} = (1-x_w)\,[2C(x_w)]^{\frac{1}{2}}$. Dashed curves correspond to the analytical bounds (4.17).

When x decreases, the angle between ray S and axis P in figure 4 grows and tends to $\frac{1}{2}\pi$ when $x_w \to -1$. Curve D in the limit merges with the vertical axis and the

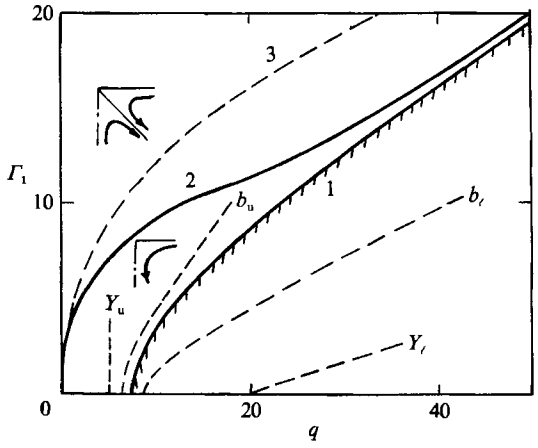

FIGURE 9. Regime map in the free-vortex problem, $x_c = 0$. Curve 1 is the existence boundary, its analytical estimates are shown by curves Y_u, Y_ℓ (Yih *et al.* 1982) and b_u, b_ℓ (this work). Curve 2 separates the upward and two-cell regime regions. Curve 3 corresponds to the two-cell regime with $\theta_S = \frac{3}{4}\pi$.

segment $0 \leqslant P \leqslant 1$ of axis P. When x_w increases, ray S approaches axis P and coincides with it with $x_w \to 1$. This limit corresponds to flow in a pipe driven by a screw motion of a thin coaxial cylinder.

5.4. *A free conical vortex*

The problem is considered in the region $-1 \leqslant x \leqslant x_c$. The system (2.2), (2.5), (2.6) with boundary conditions (2.10), (2.11) is solved as follows. Integration runs from $x = -1$ to $x = x_c$. From (2.6), (2.10), (2.15) we have $F(-1) = F'(-1) = 0$. Tentative values of $F''(-1)$, $\Gamma(-1)$ and $y'(-1)$ are taken. Note that $y'(-1)$ may not be found from (2.6) and it is a free parameter. One of the parameters (usually $F''(-1)$) is chosen by shooting to satisfy $y(x_c) = 0$. The other two define implicitly the values of Γ_1 and A.

Bearing in mind possible geophysical and astrophysical applications, the case $x_c = 0$ will be studied in more detail. The regime map is shown in figure 9. To compare with earlier results (Goldshtik 1981; Yih *et al.* 1982) the parameter $q = y'(0)$ is used instead of A. It characterizes the strength of the point sink in the plane $x = 0$. The solutions exist in the region placed on the left of curve 1. Dashed curves b_u and b_ℓ correspond to analytical estimates (4.7), (4.8) (compare with the same ones by Yih *et al.*).

Curve 1 has been found numerically as a result of solving the problem (4.3). In this case $q = q_* = -\frac{1}{2}A - \frac{1}{4}\Gamma_1^2$. At $\Gamma_1 = 0$ we have the Squire problem and $q = 7.6727$ (Goldshtik 1981). When Γ_1 increases, then q grows and at $\Gamma_1 \gg 1$ there is the power asymptote $q_* \sim \Gamma_1^{\frac{4}{3}}$. To show this we note that at curve 1, equation (2.6) may, according to (2.5), (4.5), be written as

$$(1-x^2)y' + 2xy - \tfrac{1}{2}y^2 = 2b(x-x_0)(1+x). \tag{5.4}$$

When $b \to \infty$ one must have $x_0 \to 0$ for solution existence. Then in the flow core $y \approx y_p(x)$, where

$$y_p(x) = -2[-bx(1+x)]^{\frac{1}{2}}. \tag{5.5}$$

One sees that $y'_{\mathrm{p}}(x) \to \infty$ with $x \to 0$. Therefore, a boundary layer is formed near the plane $x = 0$. Introducing new variables $y = -(2b)^{\frac{1}{3}}w$, $\eta = -(2b)^{\frac{1}{3}}x$, $\eta_0 = -8(2b)^{\frac{1}{3}}x_0$, putting them into (5.4) and letting $b \to \infty$ we obtain the following boundary layer equation:

$$\frac{\mathrm{d}w}{\mathrm{d}\eta} = \tfrac{1}{2}w^2 - \eta + \eta_0, \quad w(0) = 0. \tag{5.6}$$

When $\eta \gg 1$ the equation has the asymptotic solutions $w = \pm(2\eta)^{\frac{1}{2}}$. If η_0 is chosen arbitrarily, then a solution of (5.6) asymptotes to $w = -(2\eta)^{\frac{1}{2}}$ as $\eta \to \infty$. But to agree with (5.5) it is required that $w \sim (2\eta)^{\frac{1}{2}}$ as $\eta \to \infty$.

For this η_0 must be chosen in a special way. Calculations yield $\eta_0 = 1.2836$. The velocity distribution near the plane is shown in figure 7 (curve 2). With the help of (4.4), (4.5) and (5.4) we find $q_* = y'(0) = -2bx_0 = \eta_0(2b)^{\frac{2}{3}}$, $s = 1$, $b = \frac{1}{4}\Gamma_1^2$ and finally $q_* = 0.808\,\Gamma_1^{\frac{4}{3}}$.

Because $y_{\mathrm{p}}(x)$ does not satisfy the condition $y(-1) = -4$, a near-axis boundary layer develops. Using new variables $y = -w$, $\eta = 2b(1+x)$ in (5.4) and letting $b \to \infty$ we have

$$\eta\frac{\mathrm{d}w}{\mathrm{d}\eta} = w - \tfrac{1}{4}w^2 + \tfrac{1}{2}\eta, \quad w(0) = 4, \quad \frac{\mathrm{d}w}{\mathrm{d}\eta}(0) = \tfrac{1}{4}. \tag{5.7}$$

The latter equality follows from a regularity requirement at $\eta = 0$. The function $w(\eta)$ increases monotonically and, as $\eta \to \infty$, has the asymptote $w = (2\eta)^{\frac{1}{2}}$ according to (5.5).

Thus, for parameters Γ_1 and q corresponding to a point near curve 1 in figure 9, with $\Gamma_1 \gg 1$, the flow structure consists of (a) the inner axial layer (the Schlichting jet) with width $\sim (q_* - q)$ and velocity $\sim (q_* - q)^{-1}$, (b) the outer axial layer with width $\sim \Gamma_1^{-2}$ and velocity Γ_1^2, (c) the potential core with velocity $\sim \Gamma_1$, (d) the near-plane layer with width $\sim \Gamma_1^{-\frac{2}{3}}$ and maximum velocity $\sim \Gamma_1^{\frac{4}{3}}$.

If Γ_1 is fixed and q decreases, then the axial jet becomes wider, the minimum in the radial velocity distribution appears at the axis, at some q the axial velocity changes its sign (curve 2 in figure 9), and at the lower q values, a reverse flow develops near the axis (see the sketch in figure 9 above curve 2). There is a conical surface $x = x_{\mathrm{S}}$ separating the flow cells, and x_{S} decreases together with q. The typical curve where $x_{\mathrm{S}} = \mathrm{Const}$ ($= -0.707$) is shown in figure 9 (curve 3), and an example of the velocity distribution in the two-cell flow is shown in figure 10. In this case Γ_1 is high enough that we see the asymptotic tendency, i.e. the near-plane boundary layer with the convergent flow, the divergent conical jet near $\theta = \theta_{\mathrm{S}}$, and an almost step-like distribution of the circulation. In the near-axis region rotation is practically absent and $y \approx y'(1)(1+x)$. In view of $y(x_{\mathrm{S}}) = 0$, the flow in the region $-1 \leqslant x \leqslant x_{\mathrm{S}}$ may be considered as an autonomous problem of the same class, if $y'(x_{\mathrm{S}})$ and $\Gamma(x_{\mathrm{S}})$ are known.

Let us return to the regime map in figure 9 and note that when q tends to zero the cone $x = x_{\mathrm{S}}$ merges with the plane $x = 0$ and the flow becomes of one-cell structure. Near the symmetry axis, fluid moves towards the origin and then spreads away near the plane. The velocity distribution in this case is shown in figure 11 and a few streamlines of the meridional motion (i.e. the curves $\psi = \nu r y = \mathrm{Const}$) are shown in figure 12. There is a swirling jet fan near the plane. Outside the jet (below the dashed line in figure 12) fluid rotation is practically absent.

The fan jet has width $\sim \Gamma_1^{-1}$ with maximum velocity $\sim \Gamma_1$. Intensity of the near-axis rotation may be measured by the value of $\Gamma'(-1)$. When Γ_1 increases, then $y'(-1)$ grows and asymptotically is proportional to $\Gamma_1^{\frac{1}{3}}$, but $\Gamma'(-1)$ first grows and

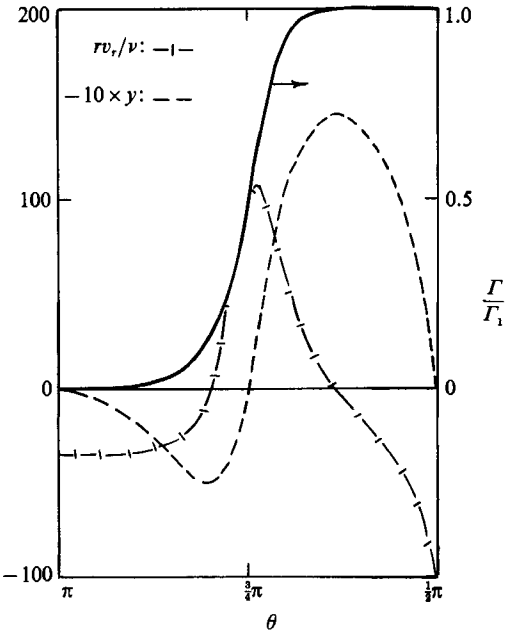

FIGURE 10. Distribution of velocity components at $\Gamma_1 = 40.7$, $q = 103.2$ ($x_s = -0.707$). The parameters correspond to a point on curve 3 in figure 9).

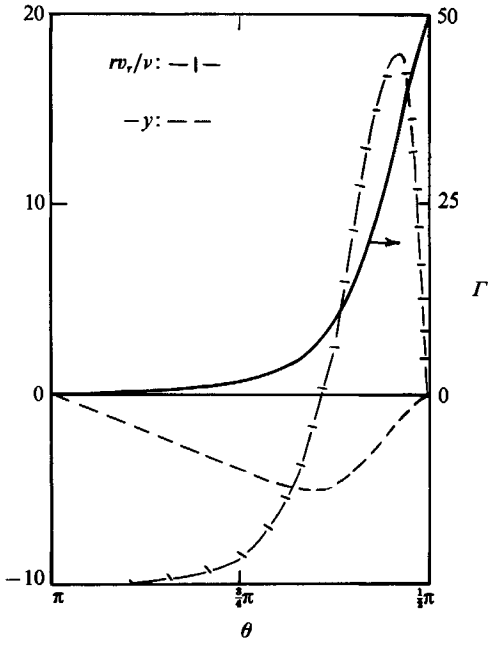

FIGURE 11. The same as figure 10 but $\Gamma_1 = 50$, $q = 0$. (The parameters correspond to the vertical axis in figure 9.)

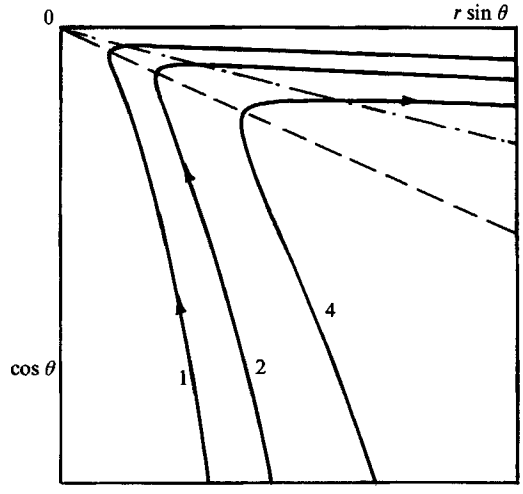

FIGURE 12. Meridional motion streamlines at $\Gamma_1 = 50$, $q = 0$ (see figure 11). The numbers 1, 2, 4 are the Stokes stream-function values in arbitrary units. On the dashed line $v_r = 0$; on the dot-dash one the distance from the plane $x = 0$ approaches the minimum.

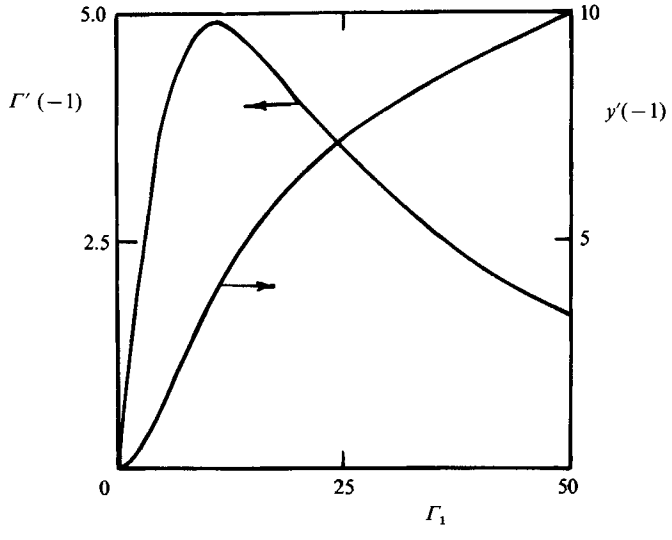

FIGURE 13. Characteristics of the radial ($y'(-1)$) and rotational ($\Gamma'(-1)$) motion near the axis versus the plane circulation at $q = 0$ (vertical axis in figure 9).

then decreases (see figure 13). Analytical estimates for $\Gamma_1 \gg 1$ (Goldshtik & Shtern 1987) provide the approximate correlation

$$\Gamma'(-1) = 2.12\Gamma_1^{\frac{3}{4}} \exp(-0.85\Gamma_1^{\frac{1}{4}}).$$

Non-monotonical behaviour of $\Gamma'(-1)$ has the same physical explanation as in the case of figure 2(*a*). The vortex line (or cone) and the vortex at the plane both induce fluid flow towards the source of rotation. This prevents vorticity diffusion from the source. As a result, the circulation is locked in a boundary layer near the source. One may say that a self-focusing of the rotation occurs. If the circulation source is a plane (or a cone), then the boundary-layer thickness decreases asymptotically as Γ_1^{-1} when

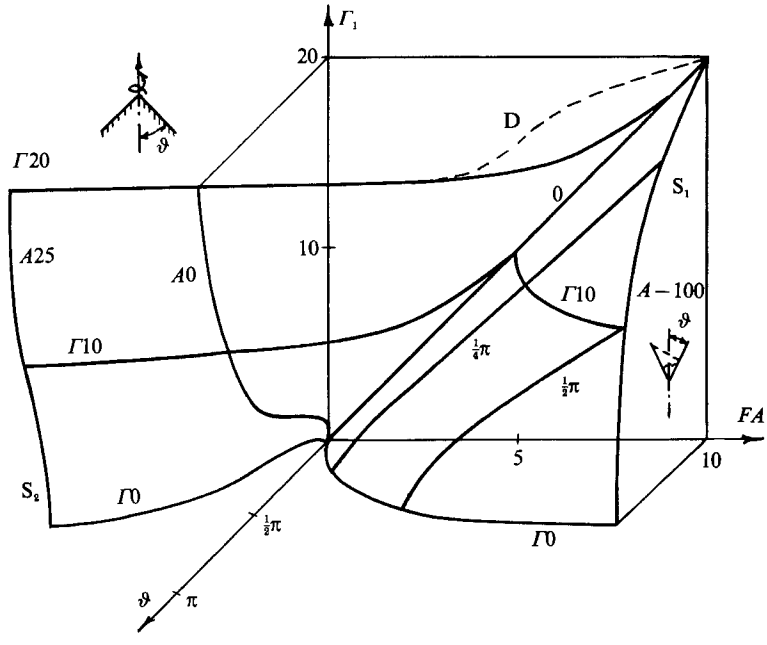

FIGURE 14. Summary picture of the solution existence boundaries in the parameter space. For comments see §5.5.

$\Gamma_1 \to \infty$, but in the case of the vortex half-line the thickness tends to zero at a finite value of Γ_1.

5.5. *Summary of the numerical results*

All our results on the solution existence loss are summarized in figure 14. Both the cases of interaction between the vortex half-line and the conical wall (see the sketch on the left and surface S_2) and the free conical vortex problem (the sketch on the right and surface S_1) are represented. The parameter $FA = -|A|^{\frac{1}{2}} \operatorname{sign}(A)$ is used instead of A to make the diagram compact.

Surfaces S_1 and S_2 are marked by the curve families $\vartheta = \text{Const}$ ($0, \frac{1}{4}\pi, \frac{1}{2}\pi$, with the same symbols near the curves), $\Gamma_1 = \text{Const}$ ($0, 10, 20$ on curves $\Gamma 0$, $\Gamma 10$, $\Gamma 20$) and $A = \text{Const}$ ($25, 0, -100$ on curves $A25$, $A0$, $A-100$). Curve 0 ($\vartheta = 0$, $\Gamma_1 = FA$) is common to S_1 and S_2.

The region of solution existence for the problem on the free conical vortex is to the left of surface S_1. At the parameter values corresponding to S_1, a sink singularity appears on the free (lower) half-axis. Plane $\vartheta = 0$ is a boundary of the existence region too. There the sink appears on the upper half-axis. On curve 0, being the common part of the boundaries, a regular solution may exist.

For the vortex–wall interaction problem the boundary is more complex. For A positive, solutions exist in the region to the right of S_2. But for $A < 0$ ($FA > 0$) in the region contained between S_2 and surface D (the latter is shown only by its trace on plane $\Gamma_1 = 20$, see dashed curve D) two regular solutions coexist. At surface D, which is bounded by curves $A0$ and 0, the solutions merge and disappear. One of these solutions with a two-cell structure loses its existence, when a parameter point touches surface S_2 from the left-hand side. The existence loss at surface D is not related to singularity appearance. Surface S_2 is the parameter set at which the sink

singularity is formed in the vortex half-line. Plane $\vartheta = 0$ is also on the existence region boundary. If Γ_1 and $FA > \Gamma_1$ are fixed, but the angle ϑ of the conical wall decreases, then the sink is generated at the lower half-axis in the limit $\vartheta \to 0$.

6. Discussion

6.1. *Ways of overcoming the paradox*

The phenomenon of vorticity concentration in thin layers and the formation of strong jets has a clear physical background. It consists in the opposite action of convection and diffusion and the predominance of convection at high velocity. But the fact that the layer thickness tends to zero and the jet momentum becomes infinite at finite values of parameters characterizing the motion drivers, i.e. what we call the collapse phenomenon, seems to be paradoxical. In real flows velocities remain, surely, bounded in this situation, and the paradox means that the mathematical models of these natural processes considered cease to be adequate. In this sense the problem of overcoming the paradox includes the study of what modification to the problem formulation is needed to re-establish solution existence.

Certainly, all the conically similar solutions have a singularity at the origin. But in this context, that seems to be not important because the solution may be considered as the main part of an asymptotic expansion with respect to r/r_0, where r_0 is a scale length of some regularization near the origin. In the case of collapse the sink singularity is formed on a half-axis, i.e. arbitrarily far from the origin too. That is why we think the origin regularization may not serve as the main way of overcoming the paradox.

There are three different cases of existence loss in these problems. The first is the generation of an additional singularity at the vortex line. The second is the merging of two smooth solutions. The third is the singularity appearance on the free half-axis.

In the first case the paradox may be resolved in the same solution class. The vortex line is an idealization of some real source of motion, for example, a rotating needle or tornado core. It has been shown that it is sufficient to replace the vortex half-line by a narrow vortex cone, and then the solution exists at any finite parameter values.

Serrin (1972) suggested another way of avoiding the paradox. He introduced a new parameter P characterizing an additional logarithmic singularity at the axis, and then the following selection principle was claimed. At any fixed circulation value the parameter P is chosen as 1 (in this case the logarithmic singularity is absent) or, if it is impossible, then P is chosen to be as close to 1 as possible. But the physical reason for this selection is not clear enough. The vortex line in the Serrin problem serves as a source not only of the angular momentum but of the axial momentum too. Both the sources may be characterized by independent parameters, and each source may drive a fluid motion separately. The selection of the one-parameter solution family is not needed because replacing the vortex half-line by an arbitrary narrow cone leads to solution existence at any parameter values. Moreover, in some parameter subregion the solution is not unique.

Now we turn to the second case – the existence loss caused by solution merging. This case is robust or structurally stable. The existence loss is preserved under a small modification of the problem formulation, and in particular on replacing the vortex half-line by a narrow vortex cone. What happens if one changes the parameters continuously, so that a marking point passes through curve D in figure 4, for instance, when the circulation is fixed and P increases (figure 5)?

The answer becomes obvious after the vortex line – cone replacement. In the case

of the cone we have a well-known hysteresis phenomenon (figure 5) or the 'fold catastrophe' (Arnol'd 1984). If the vortex line problem is considered as the limit of the vortex cone problem, when x_c tends to 1, then ray S for $P < 1$ in figure 4 may also be interpreted as a fold line. In this case the third solution is singular, with the axial sink reported in §§5.1, 5.2. For $x_c < 1$ the part of the ray S with $0 < P < 1$ transforms into a regular fold line, and the other part of S (with $P > 1$) ceases to be the solution existence boundary. The fold curves D and S meet and disappear at the cusp point $P = 1$, $\Gamma_1 = \Gamma_*$. This catastrophe may be physically meaningful, and it will be discussed further.

In the third case, when the sink singularity happens at the free half-axis, the paradox cannot be overcome or interpreted within the framework of the solution class studied. Singularity appearance at an internal point of the region or, physically speaking, a viscous collapse of vorticity, seems itself to be an unusual and strange phenomenon. In some sense it is like a cumulative effect of jet collision. Here it is the case when one of the possible ways of overcoming the paradox is a singularity regularization at the origin. It is not excluded that at supercritical parameter values the main term of an asymptotic expansion corresponds to slower decrease than r^{-1}. Such a situation is usual for wakes. To test this conjecture a rather sophisticated mathematical analysis is needed. Another possibility is that the existence loss is preceded by instability and turbulence development. Instability seems to be quite probable, because the strong jets generated before the existence loss are usually unstable at low Reynolds numbers owing to inflection points of the velocity profile. Formulation of the stability problem for solutions of the conical class is still lacking, and it calls for a special study. A more simplified model approach has been used to avoid the existence loss in our recent work (Goldshtik & Shtern 1988, 1989). It is assumed that if the jet momentum exceeds a certain critical value then turbulence appears. The turbulence is taken into account using the Boussinesq model of eddy viscosity depending on x. It is shown that an appropriate choice of the function $\nu(x)$ allows one to avoid the solution existence loss. In the variable-viscosity problem a bifurcation of self-swirling regimes (i.e. a turbulent vortex dynamo phenomenon) was found. Returning to the present problem, we conclude that, in the third case, to overcome the paradox is not easy. It remains an open problem and it seems that rather laborious analytical and numerical investigations are needed for its solution.

6.2. *Possible applications*

A physical interpretation of the vortex line and plane interaction problem as the simplest model of a tornado has been discussed in detail by Serrin (1972). Replacing the vortex half-line by a vortex cone with a small angle does not change the interpretation. But the results obtained here concerning the non-uniqueness and hysteresis indicate a probable mechanism for the sudden appearance and disappearance of strong localized atmospheric vortices. Under the same conditions two regimes may coexist which are stable to small perturbations.

One of them (corresponding to the upper branch of the solid line in figure 5) is characterized by a downward meridional flow and a rather extended rotating motion, and the other (corresponding to the half-line $a = 0$, $P > P_S$ at $x_c = 1$ or the lower branch of the dot-dash curve at $x_c = 0.999$ in figure 5) is characterized by a strong upward jet and a localization of the rotation near the symmetry axis (compare distributions 1 and 3 in figure 6). The latter regime may be correlated with a large energy concentration in a small region that may cause catastrophic consequences. The intermediate steady solution (corresponding to the lower branch of the solid line

in figure 5) seems to be unstable. It belongs to a separatrix surface dividing the attraction basins of the stable solutions.

If the circulation is fixed, then the axial force serves as a governing factor. This force may be caused by buoyancy when the core temperature differs significantly from the ambient one. For a cold core the force acts downward and the regime is one of downward flow. Gradual increase of the core temperature (corresponding to a point on the upper branch of the solid line moving to D in figure 5) may cause the sudden generation of a tornado (the point passing through D 'falls' onto the lower branch of the dashed-dotted curve). Now let the core temperature decrease. Then at some lower temperature (corresponding to the point of the dot-dash curve fold in figure 5) the tornado suddenly disappears, and the regime becomes downward. This leads to the idea that a tornado may be destroyed by producing a strong enough downward flow in its core.

The problem of the free conical vortex also has some geophysical interpretation. When the circulation and the radial velocity are given at the plane $x = 0$, the case may be considered as a model of air motion above a whirlpool. If the radial motion of water predominates, then a strong upward air jet is generated. But when the surface circulation is large enough, a reversal of the air axial motion takes place, producing a downward flow near the axis. Such a situation is dangerous not only for ships but for airliners too.

The same solution family may model the opposite case, when a tornado placed over a water surface drives the ocean motion in the meridional structure shown in figure 12. This helps a large-scale mixing in the upper ocean layer, in addition to a turbulent transfer induced by wind waves. One more application of the Squire solution (without circulation) was reported by Wang (1971) to model a water flow induced by oil spread along the ocean surface caused by a tanker crash.

Astrophysical speculations based on the free-vortex problem seem to be tempting. Recently a variety of jet-like flows has been observed in space (Lada 1985; Henricsen 1986). The nature of the jets is an open question; moreover Lada calls these jets 'enigmatic'. The jets are observed near stars and other massive objects in their condensation stage, and are correlated with accretion disks (Königl 1986). The disks are regions of higher density than that of the ambient molecular gas. The disk matter flows towards a mass centre because of the gravitational attraction.

If the accretion disk is idealized as a material plane and the massive object as a sink, then we have the Squire problem and its generalization for swirling flows. In this model the plane-matter motion drives two bipolar jets in an ambient medium with the help of viscosity. The jet may be arbitrarily strong even at rather slow disk-matter motion. Such an effect is a direct consequence of the Navier–Stokes equations. Suppose that at the first stage of the gravitational condensation the radial motion predominates over the rotational one. Then the bipolar jets may have a large axial momentum but a weak swirl velocity. This corresponds to a region near curve 1 in figure 9. If the circulation is conserved and the sink strength decreases, then the jet velocity at the axis falls from an arbitrarily large value (near curve 1) to zero (at curve 2). Further, the flow becomes a two-cell one, and when the sink strength becomes zero (i.e. the condensation is finished) the flow is reversed everywhere, and the rest of the disk mass and angular momentum are transported away by a near-plane fan jet. This may be correlated with a radial distribution of mass in planet systems and a rather complex circulation distribution in galaxies (Tayler 1978).

7. Conclusion

Let us summarize the main results of the work. Two problems have been studied by analytical and numerical methods. The first concerns a flow driven by a vortex half-line or a vortex cone in the presence of a conical wall. The second concerns a free conical vortex. A common feature of these problems is loss of existence of the solution at some finite values of parameters characterizing the motion sources. Surfaces bounding the solution existence regions in parameter space have been found. The existence loss is caused by a sink singularity appearance on the symmetry axis (collapse) or by regular solution merging (hysteresis). This is classified into three cases.

In the first case the additional sink singularity is formed at the vortex line. It may be avoided by replacing the vortex half-line by a narrow vortex cone. In the second case three solutions coexist in some parameter subregion and hysteresis takes place. In the third case the singularity appears on the free half-axis, i.e. inside the fluid flow region. Overcoming and interpretation of the latter paradox remains an open question.

Some speculations are discussed concerning possible applications of the results obtained to model such natural objects as tornadoes, whirlpools and astrophysical jets.

REFERENCES

ARNOL'D, V. I. 1983 *Catastrophe Theory*. Moscow University Press, 80 pp. (English trans. R. K. Thomas, 1984, Springer.)

BOYAREVICH, V. V., FREIBERG, YA. ZH., SHILOVA, YE. I. & SHCHERBININ, A. V. 1985 *Electrovortex Flow*. Riga: Zinatne, 315 pp.

GOLDSHTIK, M. A. 1960 A paradoxical solution of the Navier–Stokes equations. *Appl. Mat. Mech.* (*Sov.*) **24**, 610–621.

GOLDSHTIK, M. A. 1979 On swirling jets. *Mech. Fluid Gas* (*Sov.*) **1**, 26–36.

GOLDSHTIK, M. A. 1981 *Vortex Flows*. Novosibirsk: Nauka, 366 pp.

GOLDSHTIK, M. A. & SHTERN, V. N. 1987 Induced jets and critical phenomena in viscous flows. Novosibirsk: Institute of Thermophysics, preprint N 159, 50 pp.

GOLDSHTIK, M. A. & SHTERN, V. N. 1988 Conical flows of fluid with variable viscosity. *Proc. R. Soc. Lond.* A **419**, 91–106.

GOLDSHTIK, M. A. & SHTERN, V. N. 1989 On a mechanism of astrophysical jets. *Sov. Phys. Dokl.* **304**, N 5, 1069–1072.

GOLDSHTIK, M. A., SHTERN, V. N. & YAVORSKY, N. T. 1989 *Viscous Flows with Paradoxical Features*. Novosibirsk: Nauka, 340 pp.

HAMEL, G. 1916 Spiralförmige Bewegungen zäher Flüssigkeiten. *Jber. D. Mat. Verein* **25**, 334–360.

HENRICSEN, K. H. (ed.) 1986 Proceedings of conference on jets from stars and galaxies. *Can. J. Phys.* **64**, 351–535.

JEFFERY, G. B. 1915 Two-dimensional steady motion of a viscous fluid. *Phil. Mag.* **29**, 455–465.

KÖNIGL, A. 1986 Stellar and galactic jets: theoretical issues. *Can. J. Phys.* **64**, 362–368.

LADA, C. J. 1985 Cold outflows, energetic winds, and enigmatic jets around young stellar objects. *Ann. Rev. Astr. Astrophys.* **23**, 267–317.

LANDAU, L. D. 1944 On an exact solution of the Navier–Stokes equations. *Dokl. Akad. Nauk. SSSR* **43**, 299–301.

PAULL, R. & PILLOW, A. F. 1985*a* Conically similar viscous flows. Part 2. One-parametric swirl-free flows. *J. Fluid Mech.* **155**, 343–358.

PAULL, R. & PILLOW, A. F. 1985*b* Conically similar viscous flows. Part 3. Characterization of axial causes in swirling flows and one-parameter flow generated by a uniform half-line source of kinematic swirl angular momentum. *J. Fluid Mech.* **155**, 359–380.

PILLOW, A. F. & PAULL, R. 1985 Conically similar viscous flows. Part 1. Basic conservation principles and characterization of axial causes in swirl-free flow. *J. Fluid Mech.* **155**, 327–342.

SCHLICHTING, H. 1965 *Grenzschicht Theorie.* Karlsruhe: G. Braun, 742 pp.

SCHNEIDER, W. 1981 Flow induced by jets and plumes. *J. Fluid Mech.* **108**, 55–65.

SCHNEIDER, W. 1985 Decay of momentum flux in submerged jets. *J. Fluid Mech.* **154**, 91–110.

SCHNEIDER, W., ZAUNER, E. & BOHM, H. 1987 The recirculatory flow induced by a laminar axisymmetric jet issuing from a wall. *Trans. ASME* I: *J. Fluids Engng* **109**, 237–241.

SERRIN, J. 1972 The swirling vortex. *Phil. Trans. R. Soc. Lond.* A **271**, 325–360.

SLEZKIN, N. A. 1934 On a case of integrability of the full differential equations of viscous fluid motion. *Sci. Pap. Moskow Univ.* **2**, 89–90.

SOZOU, C. 1971 On fluid motions induced by an electric current source. *J. Fluid Mech.* **46**, 25–32.

SQUIRE, B. 1952 Some viscous fluid flow problems. 1. Jet emerging from a hole in a plane wall. *Phil. Mag.* **43**, 942–945.

TAYLER, R. J. 1978 *Galaxies: Structure and Evolution.* London and Basingstoke: Wykeham, 223 pp.

VAN DYKE, M. 1975 *Perturbation Methods in Fluid Mechanics.* Parabolic, 310 pp.

WANG, C. V. 1971 Effect of spreading of material of the surface of a liquid. *Intl J. Nonlinear Mech.* **6**, 255–262.

YATSEEV, V. N. 1950 On a class of exact solutions of the viscous fluid motion equations. *Sov. Phys., J. Exp. Theor. Phys.* **20**, 1031–1034.

YIH, C.-S., WU, F., GARG, A. K. & LEIBOVICH, S. 1982 Conical vortices: A class of exact solutions of the Navier–Stokes equations. *Phys. Fluids* **25**, 2147–2157.

ZAUNER, E. 1985 Visualization of the viscous flow induced by a round jet. *J. Fluid Mech.* **154**, 111–120.

ZUBTSOV, A. V. 1984 On a self-similar solution for weak-swirling jet. *Mech. Fluid Gas* (*Sov.*) **N4**, 45–50.